Title	Dissipative particle dynamics simulations for fibre suspensions in newtonian and viscoelastic fluids(Main article)
Author(s)	Duc, Duong-Hong; Nhan, Phan-Thien; Yeo, Khoon Seng; Ausias, Gilles
Citation	Duc, D. H., Nhan, P. T., Yeo, K. S., & Ausias, G. (2010). Dissipative particle dynamics simulations for fibre suspensions in newtonian and viscoelastic fluids. Computer Methods in Applied Mechanics and Engineering, 199(23-24), 1593-1602.
Date	2010
URL	http://hdl.handle.net/10220/6814
Rights	© 2010 Elsevier. This is the author created version of a work that has been peer reviewed and accepted for publication by Computer Methods in Applied Mechanics and Engineering, Elsevier. It incorporates referee's comments but changes resulting from the publishing process, such as copyediting, structural formatting, may not be reflected in this document. The published version is available at: [DOI: http://dx.doi.org/10.1016/j.cma.2010.01.010].

Dissipative Particle Dynamics Simulations for Fibre Suspensions in Newtonian and Viscoelastic Fluids

Duc Duong-Hong[1,2], Nhan Phan-Thien[3], Khoon Seng Yeo[4], Gilles Ausias[5]

[1] School of Materials Science and Engineering, Nanyang Technological University, N3-B4-W310 Nanyang Avenue, 639798 Singapore
[2] Abbott Vascular, 3200 Lakeside Dr., Santa Clara, CA 95054, US
[3] Chemical Engineering and Materials Science, UC Davis, 3014 Bainer Hall, CA 95616, US
[4] Department of Mechanical Engineering, National University of Singapore, 9 Engineering Drive 1, 117576 Singapore
[5] LG2M, Université de Bretagne-Sud, Rue de St-Maudé, BP 92116, 56321 Lorient Cedex, France

Abstract:

A versatile model of fibre suspensions in Newtonian and viscoelastic fluids has been developed using Dissipative Particle Dynamics method. The viscoelastic fluid is modelled by linear chains with linear connector spring force (the Oldroyd-B model), which is known to be a reasonable model for the so-called Boger fluid (a dilute suspension of polymer in a highly viscous solvent). The numerical results are in excellent agreement with the analytical results of the Oldroyd-B model in simple shear flow. An effective meso-scale model of fibre in DPD is proposed and then incorporated with simple Newtonian fluid and our Boger fluid to enable entirely study rheological properties of fibre suspensions in both Newtonian and viscoelastic solvents. The numerical results are well compared with available experimental data and other numerical models.
.

Keywords:

Simulation; fibre suspensions; Newtonian; Oldroyd-B; DPD method

1. Introduction

Rod-like particle suspensions can be found in many important applications such as carbon nanotubes and short fibre reinforced composites (SFCs). The latter is increasingly used in industrial and domestic applications because of its outstanding high strength, stiffness, toughness, and yet remains low-weight and low manufacturing cost, compared to conventional plastics. Fibre orientation, on the other hand, is a key factor controlling the properties of SFCs. It is strongly affected by the flow conditions, and not so easily predicted.

Most commercial composites commonly used in injection moulding fall into the semi- or highly-concentrated regimes and the matrix is universally a polymeric liquid [1]. In non-dilute suspension studies, particle-particle interactions must be carefully considered since they can strongly affect the fibre orientation, and hence the macroscopic properties of suspensions. Several investigations of fibre-fibre interactions have been reported (Dinh and Armstrong [2], Folgar and Tucker [3]; Yamane et al. [4-5], Phan-Thien et al. [6]). Dinh and Armstrong [2] used a

distribution function to describe the orientation state of fibres and fibre-fibre interactions are also taken into account. They derived a rheological equation of state for semi-dilute fibre suspensions. Folgar and Tucker [3] developed an evolution equation for concentrated fibre suspensions, where particle-particle interactions are taken into account by adding a diffusion term to Jeffery's equation. They assumed the diffusivity is proportional to the shear rate. The constant of proportionality, which is known as the Folgar-Tucker constant C_i, was determined empirically. Phan-Thien et al. [6] suggested an empirical equation to calculate C_i for a fibre suspension in a Newtonian fluid, based on their numerical modelling. However, their theory was also based on Newtonian suspension.

Compared to numerous studies of Newtonian fibre suspension, there are relatively fewer works done on viscoelastic fibre suspensions. The effect of non-Newtonian fluid on the orientation of a single particle was studied by a number of authors ([Joseph and Liu [7], Iso et al. [8][9], Phan-Thien et al. [10]). Iso et al. [8][9] found that the fibre orientation depends on the fibre content but also the elastic properties of matrix. Phan-Thien et al. [10], using CDL-BIEM (completed double-layer boundary integral equation method), have simulated the mobility problem of a single particle in an unbounded Oldroyd-B fluid. They claimed that the method can generate accurate results; however it requires the unrealistic computational demands for a large number of fibres at the time being. This problem should be overcome by more powerful computer or the potential grid computation in future.

The fibre-suspended fluids in question are shear thinning, so that the shear viscosity decreases with increasing shear rates. Some modelling effort has been directed to this problem (Chan et al. [11]; Ganani and Powell [12]; Azaier [13]; Ramazani et al. [14][15]; Sepehr et al. [16]). Azaier [13] successfully simulated fibre suspensions in polymeric liquids modelled by different models (FENE-P, FENE-GR and Giesekus models), their numerical results showed that the ratio of the suspension viscosity and the solvent viscosity is almost constant over whole range of shear rates even at high shear rates that is not observed in several other experiments done by Chan et al. [11], Ganani and Powell [12] and Ramazani et al. [15]. Recently Ramazani et al. [15] have suggested a model incorporating a sophisticated formula of Folgar and Tucker for the parameter C_i, which is now dependent on the shear rate, the fibre orientation, the inherent fibre-fibre

interaction as well as the fibre-matrix interaction. Their experimental data and numerical results agree well, but not for small aspect ratios. The results clearly showed that at low shear rates, increasing volume fractions and/or fibre aspect ratios leads to increase the viscosity, whereas at high shear rate the suspension viscosity approach to that of suspending viscoelastic fluids and almost independence of fibre characteristics. More recently, Sepehr et al. [16] have done some experiments of fibre suspended into both Newtonian and Boger fluids. The results show that shear thinning behaviour occurs strongly in Boger solvent but is only lightly observable in Newtonian solvent and the suspension viscosity seems to approach that of the suspending viscoelastic fluid at very high shear rates.

Even in the manufacture of fibre reinforced composites, some models of fibre suspensions in Newtonian fluids are used under certain acceptable degree of accuracy. The need for more reliable models of fibre suspensions in viscoelastic fluids is clearly there. Numerical simulations should be a good choice to deal with these complicated problems. However, the computational effort required is very great indeed owing to the inherently complex behaviour of fibres in viscoelastic fluid media. An effective model of fibre suspension is therefore necessary for accurately predicting its rheological properties which is also our ultimate aim of this paper.

The Dissipative Particle Dynamics (DPD) method [17] has been developed since 1992 as a particle-based mesoscopic simulation technique. The most advantage of DPD is the easy model of complex fluids at a reasonable computational cost. Some significant successes have been achieved so far with the DPD method, e.g., in suspensions [18][19][20], micro- and nano-fluidic [21][22], and especially with diluted polymer solutions [23]-[25]. Some models of rod-like particles have been introduced by Martys and Mountain [26] and Yamamoto and Matsuoka [27][28]. Those models may provide an accurate solution, however they are still required intensive computation particularly for simulating suspensions of short-fibre at non-dilute regimes. More discussions will be presented in Section 2.2.

As an attempt to simulate fibre suspensions in wide range of concentrations, we present here an effective model for short-fibre suspensions in both Newtonian and viscoelastic fluids. The fibre-solvent and fibre-fibre interaction forces are studied in detail and then applied for different concentrated fibre suspensions in a

Newtonian fluid. Numerical results in Couette flow are validated against available experimental data [12], and also with other models. A model of Boger fluid is suggested and the results are in excellent agreement with Oldroyd-B model under Couette flow. The fibre model is further integrated with the Boger fluids for modelling fibre suspensions in viscoelastic liquids. The rheological properties of such viscoelastic fibre suspensions under Couette flows are investigated for the effect of fibre contents and different matrixes; the results are reported and compared with available data. For speed up the computation, a parallel program is introduced, and some discussions on the speed-up and efficiency are also presented.

2. DPD method and model of fibre in DPD

2.1 *DPD method*

The classical DPD method represents the flowing fluid (or deforming material) by an ensemble of interacting particles under the influence of external forces [17]. Every DPD particle is defined by its position, velocity and mass. The motion in time of a DPD particle i is obtained by integrating the following system of equations:

$$\begin{aligned} \frac{d\mathbf{r}_i}{dt} &= \mathbf{v}_i, \\ \frac{d\mathbf{v}_i}{dt} &= \sum_{j\neq i} \mathbf{f}_{ij} + \mathbf{F}_e, \end{aligned} \tag{1}$$

where the subscripts i and j range over all DPD particles. Here, we assume the mass of particles is identical and normalized to unity; $\mathbf{r}_i$ and $\mathbf{v}_i$ are the position and the velocity vectors of particle i, $\mathbf{F}_e$ is the external force, $\mathbf{f}_{ij}$ is the inter-particle force exerted on particle i by particle j, and this consists of three components: conservative, dissipative and random forces [29][30].

The conservative force, $\mathbf{F}_{ij}^C$, is given by

$$\mathbf{F}_{ij}^C = \begin{cases} a_{ij}(1 - r_{ij}/r_c)\hat{\mathbf{r}}_{ij} & (r_{ij} < r_c), \\ 0 & (r_{ij} \geq r_c), \end{cases} \tag{2}$$

where a_{ij} is the maximum repulsion between particles i and j, $\mathbf{r}_{ij} = \mathbf{r}_i - \mathbf{r}_j$, $r_{ij} = \left|\mathbf{r}_{ij}\right|$, $\hat{\mathbf{r}}_{ij} = \mathbf{r}_{ij} / r_{ij}$ is the unit vector directed from particle j to i, and r_c is a cut-off radius, here normalized to unity.

The dissipative force, $\mathbf{F}_{ij}^D$, and the random force, $\mathbf{F}_{ij}^R$, are

$$\mathbf{F}_{ij}^D = -\gamma\omega^D(r_{ij})(\hat{\mathbf{r}}_{ij} \cdot \mathbf{v}_{ij})\hat{\mathbf{r}}_{ij}, \tag{3}$$

and

$$\mathbf{F}_{ij}^R = \sigma\omega^R(r_{ij})\theta_{ij}\hat{\mathbf{r}}_{ij}, \tag{4}$$

respectively, where $\mathbf{v}_{ij} = \mathbf{v}_i - \mathbf{v}_j$, and γ and σ are the coefficients characterizing the strengths of the dissipative and random forces respectively, ω^D and ω^R are the weight functions that vanish if $r_{ij} \geq r_c$, and θ_{ij} is a white noise with the properties:

$$\left\langle \theta_{ij}(t) \right\rangle = 0 \text{ and } \left\langle \theta_{ij}(t)\theta_{kl}(t') \right\rangle = (\delta_{ik}\delta_{jl} + \delta_{il}\delta_{jk})\delta(t - t'). \tag{5}$$

To satisfy the detailed balance* [29][31], akin to the *equi-partition* principle, the weight functions obey a relation similar to the fluctuation-dissipation theorem,

$$\omega^D\left(r_{ij}\right) = \left[\omega^R\left(r_{ij}\right)\right]^2 \quad \text{and} \quad \gamma = \frac{\sigma^2}{2k_BT}, \tag{6}$$

where k_BT is the Boltzmann temperature. Fan et al. [32] recently have suggested the weight function:

$$\omega^D\left(r_{ij}\right) = \left[\omega^R\left(r_{ij}\right)\right]^2 = \begin{cases} \sqrt{1 - r_{ij}/r_c} & r_{ij} < r_c, \\ 0 & r_{ij} \geq r_c. \end{cases} \tag{7}$$

The equations of motion (1) are solved by using the velocity-Verlet algorithm suggested by Groot and Warren [30]. The stress tensor in DPD is typically calculated using the Irving-Kirkwood model [33]:

$$\begin{aligned} \boldsymbol{\sigma} &= -\frac{1}{V}\left[\sum_i m\mathbf{u}_i\mathbf{u}_i + \sum_i\sum_{j>i}\mathbf{r}_{ij}\mathbf{f}_{ij}\right] \\ &= -n\left\langle \sum_i m\mathbf{u}_i\mathbf{u}_i + \sum_i\sum_{j>i}\mathbf{r}_{ij}\mathbf{f}_{ij} \right\rangle, \end{aligned} \tag{8}$$

* A system is said to obey the detailed balance if the probabilities of motion between two microstates of the system at equilibrium are the same in each direction.

where n is the number density of particles, $\mathbf{u}_i = \mathbf{v}_i - \overline{\mathbf{v}}(\mathbf{x})$ is the peculiar velocity of particle i, with $\overline{\mathbf{v}}(\mathbf{x})$ being the flow velocity at position $\mathbf{x}$, and $\langle \bullet \rangle$ as usual denotes the ensemble average. The nice feature of DPD method is that all the average quantities, density, linear momentum, etc., satisfy all the familiar conservation laws of continuum mechanics, and DPD may also be regarded as a statistical technique for solving continuum-type problems.

2.2 *A fibre model in DPD*

In general, a rigid body in DPD is approximately modelled by a set of 'frozen' particles where the particles are fixed in positions (Koelman and Hoogerbrugge [18]; Martys and Mountain [26]). The technique has been developed for successfully modelling a rigid wall using multi layers (Fan et al. [32]; Revenga et al. [34]; Duong-Hong et al. [35]). Those techniques are reasonably applied for static objects, but dynamic one since it is extremely difficult to maintain the complex structures (multi layers). Simulating the motion of an arbitrary-shape rigid object in a general flow is still a challenging problem itself. Recently, Martys and Mountain [26], applied the frozen particle idea for rigid fibre coupled with direct approach to solve the orientation of such objects by using the quaternion equations of motions. For consistency with velocity-Verlet algorithm, they needed to translate the quaternion components into three translational degrees of freedom by adopting the Omelyan's scheme [36]; however, the computational cost increased significantly, particularly for a system of large number of fibres. Yamamoto and Matsuoka [27] suggested other methods for simulations of rigid and flexible fibres in dilute Newtonian suspensions. The fibre was modelled as a series of aligned spheres which were bonded one to another. The bond between spheres was allowed to stretch, bend and twist by changing the certain parameters of the bond distance, the bending and twisting angles, respectively. In their subsequent work, Yamamoto and Matsuoka [28] considered the hydrodynamic interaction among fibres to simulate concentrated fibre suspensions in shear flows. It is important to note that all variances of DPD particles are calculated in absolute axes whereas the inter-particle forces exert on the particle-particle axis. Therefore, it may be very expensive computationally to apply this method in simulations of suspensions, because of the complex updating scheme, where we need to alternate

between the relative axes fixing in each fibre and absolute axes in every time step for all the components (velocities, forces). It is noteworthy that those techniques may provide good solution for fibres of large aspect ratio due to the high accuracy of the algorithm. However, for short-fibre at non-dilute regimes, where the Brownian forces and the stochastic fibre-fibre interaction forces are significant, it may be very expensive to obtain an accurate solution from the algorithm.

As an attempt to simulate fibre suspensions in different concentrations, we present here an effective model, which is based on the method of Lagrange multiplier [1], for short fibres in DPD fluids.

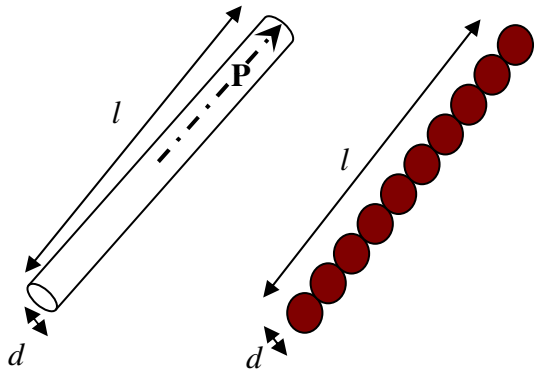

Fig. 1. The osculating multi-bead rod model

The fibre is modelled by the osculating multi-bead rod as depicted in Fig. 1, where **P** is the unit vector along the axis of fibre. Owing to the 'soft' character of repulsive forces in DPD, the distance between the adjacent beads is chosen to be quite close preventing other particles from passing through. However, the number of beads represented by a fibre should be as small as possible to reduce the computational cost. Furthermore, short-range interaction force between fibres is incorporated into simulations to prevent fibre crossing each other.

In this model, the "degree of rigidity" of a fibre is defined by the relative distances between particles in a fibre system,

$$\left|\mathbf{r}_i - \mathbf{r}_j\right|^2 = d_{ij}^2, \tag{9}$$

where d_{ij} is an original distance between particle i and j.

Note that using triangulation, angle constraints can be adequately substituted by distance constraints. Assuming there is a total of n_c distance constraints imposed

on a fibre, and if the k^{th} constraint acts between particle $i(k)$ and $j(k)$, then the constraint equations are of the form:

$$\chi_i \equiv \mathbf{r}_{i(k)j(k)}^2 - d_{i(k)j(k)}^2 = 0,\ k = 1,...,n_c. \tag{10}$$

The effect of the constraints on particle i can be regarded as the additional force-like term, namely $\mathbf{G}_i$, then the equation of motion, Eq. (1), becomes:

$$\frac{d\mathbf{v}_i}{dt} = \mathbf{F}_i + \mathbf{G}_i, \tag{11}$$

where $\mathbf{F}_i$ is the usual non-constraint forces and the additional constraint force on the i-th bead is separately considered as:

$$\mathbf{G}_i = -\sum_{k \in C(i)} \xi_k \nabla_i \chi_k. \tag{12}$$

Here $C(i)$ denotes the set of constraints that directly involve particle i and the $\{\xi_k\}$ are the Lagrange multipliers introduced into the problem. There are two approaches [37] to solve the constraint problem. In the direct approach, a matrix equation of constraint force is formed and solved for the Lagrange multipliers, and then these values are applied into the equations of motion (11). As we are modelling short fibres, the number of constraints is quite small. Therefore, the resulting linear problem can be effectively solved by using the simple LU decomposition technique [38]. This approach can render accurate result if the variance between the current positions of beads forming a rod and its original straight line is small. It therefore usually requires a small time step in implementing this method. In the alternative approach, the constraint force $\mathbf{G}_i$ is first ignored so Eq. (1) is easily computed as usual as the unconstrained systems. The constrained coordinates are then adjusted to satisfy the constraints in the next time step. This adjustment is effectively carried out by an iterative relaxation procedure [37]. In this routine each pair of constrained coordinates is modified in turn until all the constraints satisfy $\left|\mathbf{r}_{ij}^2 - d_{ij}^2\right| \le \varepsilon_r d_{ij}^2$, where ε_r is a real number representing the specified tolerance. The tolerance ε_r can represent the flexibility of fibre, for instant a small value of ε_r, i.e. 10^{-5}, is sufficient to model rigid fibres but a larger value can be used for the case of flexible fibres. The case for flexible fibres is outside the scope of this article. In general, the constrained coordinates can be effectively solved particularly for short fibres since the number of

constrains is small, so it can efficiently apply large time step of typical DPD method. In our simulations, both approaches are alternatively implemented for certain time steps to minimize the computational time yet still assure the accuracy of numerical results.

Care must also be taken in calculating the interactions between the particle beads of the fibres and solvent particles as well as between fibre beads themselves in the case of non-dilute suspensions. Since DPD method is a mesoscopic simulation technique, the interaction forces are neither the atomic forces in Molecular Dynamics [37], nor the forces in the macroscopic point of view. However, they may be determined to yield the correct the macroscopic hydrodynamic drag forces.

The problem of a single cylindrical rod (modelled as a prolate spheroid) moving with velocity **U** in a sea of Newtonian fluid is well known and the analytical solutions for the drag force coefficients are available in the literature [39]. In particular, the relationship between the force **F** and the translation velocity **U** is described by:

$$\begin{aligned} F_x &= -\frac{32\pi(1-\nu)abc\mu U_x}{(3-4\nu)\chi_o + \alpha_0 a^2}, \\ F_y &= -\frac{32\pi(1-\nu)abc\mu U_y}{(3-4\nu)\chi_o + \beta_0 a^2}, \\ F_Z &= -\frac{32\pi(1-\nu)abc\mu U_Z}{(3-4\nu)\chi_o + \gamma_0 a^2}, \end{aligned} \tag{13}$$

where a, b, and c are radii of the prolate object/spheroid as in the three principal axes, μ is viscosity of solvent, and ν is a Poisson constant, and for the prolate spheroids ($r = a/c > 1$):

$$\begin{aligned} a^{-2}\chi_o &= \frac{2}{r(r^2-1)^{1/2}} \log\left(\frac{1}{r-\sqrt{r^2-1}}\right), \\ \alpha_0 &= \frac{2r}{\left(r^2-1\right)^{3/2}} \log\left(\frac{1}{r-\sqrt{r^2-1}}\right) - \frac{2}{r^2-1}. \end{aligned} \tag{14}$$

For the case of a rod being aligned along the flow direction and moving with velocity $\mathbf{U} = (U_x, 0, 0)$, the drag force coefficient is given by:

$$\zeta_{//} = \frac{F_x}{U_x} = -\frac{32\pi(1-\nu)abc\mu}{(3-4\nu)\chi_o + \alpha_0 a^2}. \tag{15}$$

Replacing the Poisson constant $v = 0.5$ for an incompressible Newtonian medium, and applying for the rod: $a_R = r = a/c = l/d$, $d = 2b = 2c$ and $l = 2a$, we obtain:

$$\zeta_{//} = \frac{F_x}{U_x} = -\frac{8\pi l\mu}{\left[\frac{2(2a_R^{\,2}-1)}{a_R(a_R^{\,2}-1)^{3/2}}\log\left(\frac{1}{a_R-\sqrt{a_R^{\,2}-1}}\right)-\frac{2}{a_R^{\,2}-1}\right]a_R^{\,2}}. \qquad (16)$$

When the rod is moving transverse to the flow, the drag force coefficient in this case, $\zeta_\perp$ follows [41]:

$$\zeta_\perp = 2\zeta_{//}\ . \qquad (17)$$

The so-called single-rod problem customarily used to find the mesoscopic parameters. In this problem, the fibre of interest is subject to uniform channel flow of a solvent. The channel is confined between 2 walls in z direction and periodic boundary conditions are applied in x and y directions. The walls are moved with the velocity U_{wall} in x direction to generate the uniform flow of the solvent in that direction. Both cases of fibre aligned with and transverse to the flow are numerically simulated by the DPD model to determine the drag forces F_x involved and their corresponding drag coefficients computed by:

$$\zeta_{cal} = \frac{F_x}{U_{wall}}. \qquad (18)$$

The fibre parameters are chosen methodically so that the DPD-simulated drag force coefficients match the theoretical values given by Eqs. (16-18).

We applied the above procedure to find the parameters for a fibre of aspect ratio 7.63. The fibre is formed by 14 beads and the bond-length between adjacent beads is chosen to be 0.2 and it follows that the diameter of the fibre is 0.367. It is necessary to note that the larger the number of beads forming a fibre, the longer the time for computing the constraints. However, we should not choose the bond-length too large to prevent two fibres from passing through each other. Based on Groot and Warren [30], the maximum repulsion between fibres and solvent particles can be assumed at 2.15 for the case where the suspending media is a good solvent. Furthermore, since the fibre is modelled by one layer of particles hence the no-slip boundary condition on the fibre surface needs to be validated. It can be tested by implementing two-dimensional single fibre (fluid flows through a static fibre) then the velocity profile around the fibre has been investigated

through a very fine grid of bins. We observed an area around fibre particles of which velocity is almost zero. The width of this area mostly depends on the repulsive force between fibre and fluid particles.

The last parameter needed to be determined is the noise amplitude between fibres and solvent particles, the so-called σ_{RF}. This parameter is varied in several simulations: when the rod is parallel to the flow, $\zeta_{cal}^{//}$ and $\psi_1 = \frac{\zeta_{cal}^{//}}{\zeta_{//}}$ are calculated, and when the rod is transverse to the flow, $\zeta_{cal}^{\perp}$ and $\psi_2 = \frac{\zeta_{cal}^{\perp}}{\zeta_{//}}$ are calculated. The proper value for σ_{RF} is found when the conditions of $\psi_1 = 1$ and $\psi_2 = 2$ are satisfied.

Fig. 2 shows how ratios ψ_1 and ψ_2 changes with σ_{RF}; note that the σ_F is the solvent-solvent noise amplitude and fixed at the value of 3.0 suggested by Groot and Warren [30]. The best choice for σ_{RF} can then be determined by finding the crossing point between the curves of ψ_2 and $2\psi_1$. Since DPD parameters are measured in a statistical manner, an exact value is not expected. The best value for σ_{RF} is found to be 2.15 by carrying out some more simulations in the vicinity of the intersection point. It is important to note that even those parameters are found by a single rod problem, they are still reasonable to be applied for N-fibre systems since we assume that the fibres are always surrounded by the fluid (diluted solution). In highly concentrated fibre suspensions (Ausias et al. [40]), fibre-to-fibre contact may occur. This is beyond the scope of our study. In fact, they are rarely observed in our simulations hence the contact force is not considered in all our simulations.

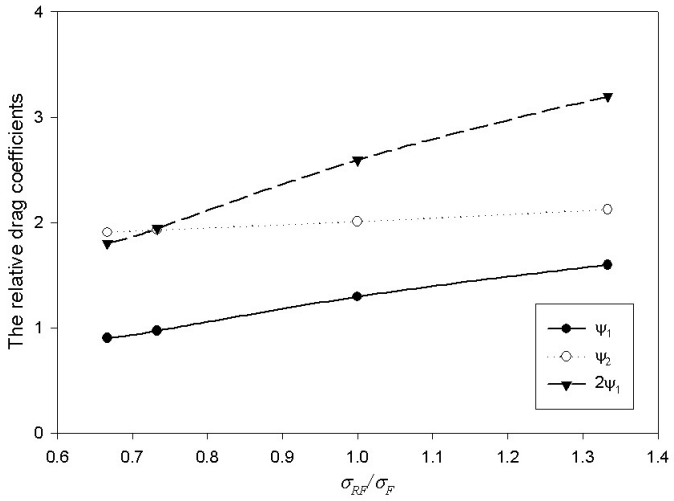

Fig. 2. The relative drag coefficients versus relative σ_{RF}/σ_F

In general, numerical simulations of a non-dilute fibre suspension are reliable only if fibre-fibre interactions are properly taken into account. The fibre-fibre interactions can be classified into two types: short-range and long-range interactions. The short range is considered when fibres come into near contact with each other. In our simulations, apart from the three inter-particle forces typically defined in DPD, which can be considered to be long-range interaction, short-range interaction between fibre particles may be handled by the method described by Yamane et al. [5]. In Yamane et al.'s treatment, *lubrication* forces between two beads of different fibres are calculated only if the distance between them is below a critical value, say 10% of the fibre diameter. Short-range interaction can significantly affect the orbit of an individual fibre when this fibre is in near contact with others. However, it rarely happens even for semi-concentrated fibre suspensions. Several simulations for different concentrated fibre suspensions in a Newtonian fluid are carried out and the results are validated with experimental data. The DPD fibre parameters are further exploited for the simulations of fibre suspensions in viscoelastic fluids, and the results are compared with other experimental data in section 3.

2.3 *Parallel programme*

The DPD algorithm can be effectively parallelized to speed up the computation for feasibly simulating large systems of fibre suspensions (large fibre aspect ratios and large channels). The Message Passing Interface (MPI) is used to implement and the programme are validated in both cluster supercomputers and grid

computations. The concepts of parallel computation are some how straightforward due to the fact that the interaction forces are limited within a defined cut-off radius, r_c.

The computational domain is first divided into several sub-domains corresponding to the number of CPUs, denote n_{CPU}, as in Fig. 3. In fact, the interaction forces are merely considered within a cut-off radius around the particular particle, therefore only particles that are near the boundary of two adjacent sub-domains need to be considered for the interactions with both the particles in its sub-domain and the particles in the neighbouring sub-domain, as described in Fig. 3. Therefore, we need to shift all the particles within the distance r_c from the sub-domain boundary to the neighbour CPUs as described in Fig. 4.

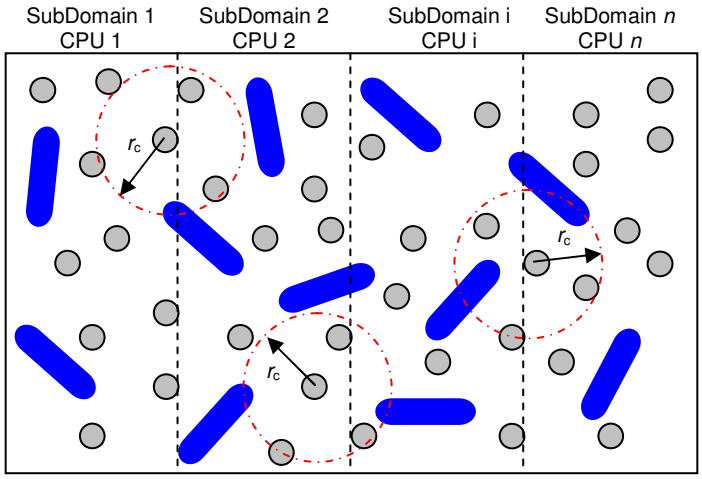

Fig. 3. The interaction forces between particles within rc

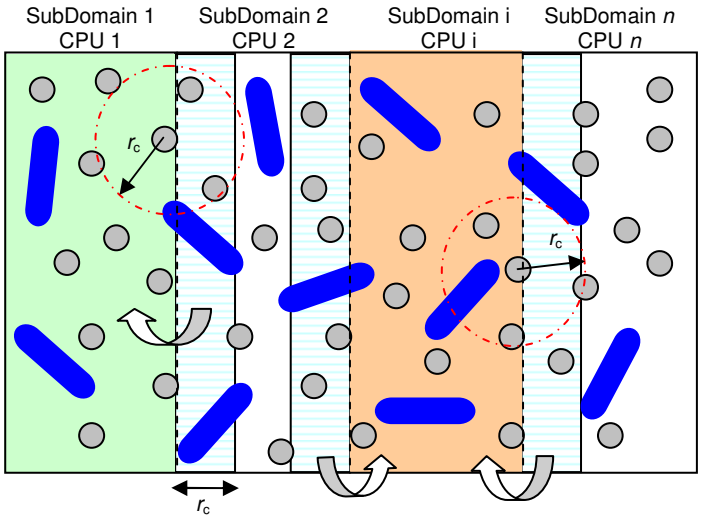

Fig. 4. The communication between sub-domains

The speed up and the efficiency of parallel algorithm are investigated for the case of 4096 fibres suspended in a Newtonian fluid contained in a channel size of 64×30×30. The results are shown in Fig. 5. Note that, the speed up is calculated by $S_n = T_1/T_n$ and efficiency is computed by $E_n = S_n/n_{CPU}$, where T_1 is the time for running a simulation using the serial program regarded as the running time using 1 CPU, and T_n is the time for a complete run of the parallel program using n_{CPU} . In Fig. 5, using 8 CPUs, the speed up seems reach the highest plateau but the efficiency reduces lower than 50%. The overall optimum performance may be estimated at using 5 or 6 CPUs.

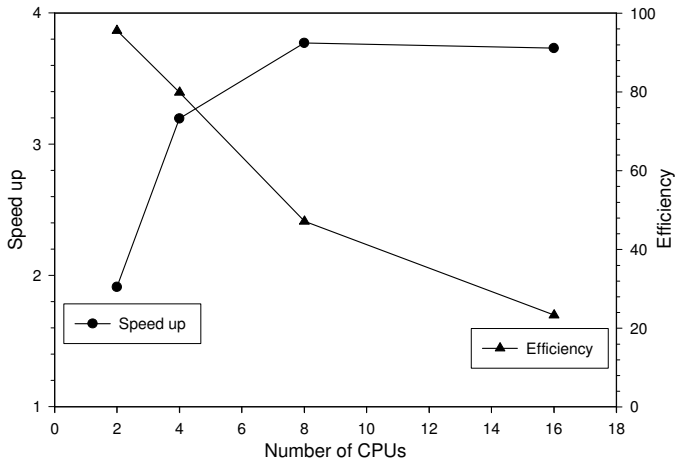

Fig. 5. The speed up and efficiency of parallel algorithm

3. Simulations and results

3.1 *Oldroyd-B fluids*

A class of real fluid can be constructed by dissolving a high molecular weight polymer solute in a highly viscous Newtonian solvent; such material is now referred to as 'Boger fluid' [41] of which properties is well presented by the Oldroyd-B model:

$$\mathbf{S} + \lambda_1 \frac{\delta \mathbf{S}}{\delta t} = 2\eta \left(\mathbf{D} + \lambda_2 \frac{\delta \mathbf{D}}{\delta t} \right), \tag{19}$$

where $\lambda_1 = \lambda$ is the relaxation time, and $\lambda_2 = \lambda\mu/\eta$ is the retardation time, and $\eta = \mu + \eta_C$ is the total viscosity where μ and η_C are the solvent viscosity and the viscosity contributed by polymer chains respectively. With $\frac{\delta \mathbf{A}}{\delta t}$ denotes the upper convected time derivative.

If the stress is expressed explicitly in the combination of solvent and the polymer stresses:

$$\mathbf{S} = \mathbf{S}^{(s)} + \boldsymbol{\tau}^{(c)} = 2\mu\mathbf{D} + \boldsymbol{\tau}^{(c)}, \tag{20}$$

then the stress contributed by the polymer can be written as the familiar upper-convected Maxwell model:

$$\boldsymbol{\tau}^{(c)} + \lambda \frac{\delta}{\delta t}\boldsymbol{\tau}^{(c)} = 2\eta_C \mathbf{D}. \tag{21}$$

In a simple shear flow and at steady state, the solution viscosity and the first- and second-normal stress differences can be calculated by:

$$\begin{aligned} \eta &= \frac{S_{12}}{\dot{\gamma}} = (\mu + \eta_C), \\ N_1 &= \tau_{11}^{(c)} - \tau_{22}^{(c)} = 2\eta_C \lambda \dot{\gamma}^2, \\ N_2 &= \tau_{22}^{(c)} - \tau_{33}^{(c)} = 0. \end{aligned} \tag{22}$$

It is apparent that the viscosity is constant over shear rates in Oldroyd-B model, but the first-normal stress difference is a quadratic function of shear rate and the second-normal stress difference is always zero.

In the literature, the polymer matrix is usually modelled by a set of DPD chains [23][24]. As usual the Oldroyd-B fluid is modelled here by a set of DPD beads threaded together in linear chain, and the interaction force between two adjacent particles, separated by a distance of x, has the potential form:

$$V = \frac{1}{2}kx^2. \tag{23}$$

A typical Newtonian fluid is usually modelled by free particles as in [17][35][29]. Particularly, the channel size is chosen at 40×10×20 in x, y, and z directions; the density of solvent is chosen at 4.0.

	Fluid name					
	F5-4	F5-12	F5-24	F2-8	F2-24	F40-4
Chain length	5	5	5	2	2	40
Mass fraction	4%	12%	24%	8%	24%	4%
H	6	6	6	2	2	2
λ	1.1	1.1	1.1	2	2	120
η_p	0.18	0.42	0.76	19.62	0.23	0.64
η_s	2.44	2.44	2.44	2.44	2.44	2.44

Table 1: The parameters of different viscoelastic fluids

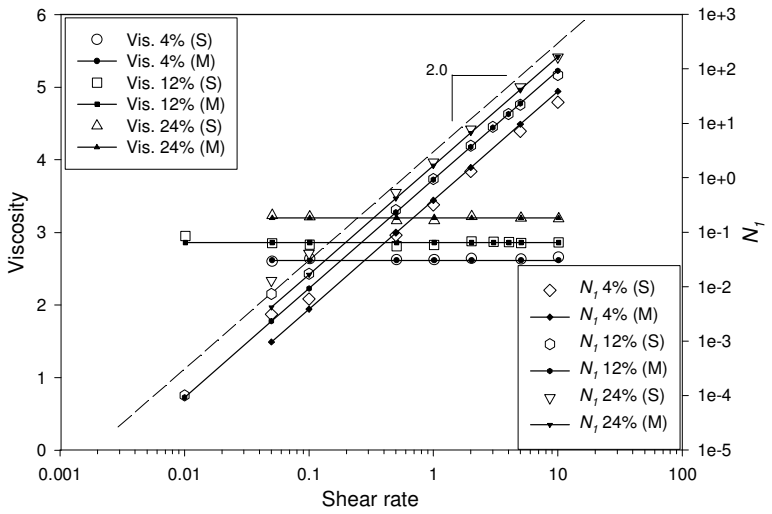

Fig. 6. The viscosity and first normal stress difference of different fluids compared very well with Oldroyd-B model. The first normal stress difference is all parallel with a line of slope of 2.0 (dash-line)

Chains of varied chain length, spring constant and mass fractions (ratio of chains and free solvent mass), tabulated in Table 1, are used to model different Boger fluids. The rheological properties of those fluids are then investigated under Couette flows and the results are compared with Oldroyd-B model.

The spring constant should be chosen in such a way that the distance between 2 adjacent chain-beads is relatively close to the distance of free particles. If the spring constant is increased, the chain is stiffer, then it may lose some basic conformational morphology. Otherwise, if the spring force is too weak, the adjacent chain-beads are largely separated, then the chains can cross over unexpectedly that may be unphysical. Groot and Warren [30] suggested the value of spring constant is about 2.0 for investigating a polymer system at the equilibrium state of static flow. However using this value, we observed that the chains are extremely stressed out, particularly for long chains, under shear flows at our considered shear rates range (0.01-10). Thus the spring constant of 6.0 is a reasonable choice, where the distance between two adjacent beads of chains is lightly less than r_c over the shear rate range. Even a proper spring constant and repulsive force parameters between chain-particle is chosen, there is no other mechanical implementation to prevent the chains from crossing one to another, therefore the chains are still regarded as 'phantom' chains.

Shear flows for the fluid with the chains are then simulated to yield the viscosity, first and second normal stress difference. The results are in excellent agreement

with Oldroyd-B model and plotted in Fig. 6, note that the second-normal stress different is almost zero (the values are about 10^{-4} ~ 10^{-3} for shear rate of 0.1 and 10 respectively – about one-order magnitude less than N_1); they are not shown in Fig. 6 for the sake of clarity.

We also simulate other fluids of different chains lengths, particularly 2 to 40 bead chains. The results of viscosity and normal stress differences are also in good agreement with Oldroyd-B model. The relaxation time is consistent with the chain length, we observe that a longer relaxation time is obtained with longer chain lengths. In Table 1, it also clearly shows that the same chain length has the same relaxation time, and the viscosity contributed by polymer is directly proportional to the mass fraction of polymer (if the mass of the solvent and polymer particles are the same, mass fractions are the same as volume fractions) while the solvent particles produces the same viscosity of Newtonian fluids [35]. It is necessary to note that the stress of polymer chains created by the spring force among chain particle can be separately considered by Irving-Kirkwood model [33]. Thus the stress of entire systems calculated by Eq. (8) is exactly the summation of the stress of generic DPD particles (Newtonian) and stringed DPD particles (Maxwell).

3.2 *Fibre suspensions in a Newtonian fluid*

A Newtonian fluid can be modelled by free particles in the original DPD method, where the parameters are suggested by Groot and Warren [30]. This fluid is well examined in our previous work [35] for both Poiseuille and Couette flows in a channel confined by two rigid walls in the z-direction and periodic boundary conditions are applied in the x and y directions. Couette flow is modelled by sliding walls, where opposite-direction velocities are applied. To prevent large density fluctuations near the wall, the wall treatment reported by Duong-Hong et al. [35] is used in all the simulations. The 938, 1877, 4693 and 7509 fibres, corresponding to the volume fractions, ϕ, of 1%, 2%, 5% and 8% respectively, are suspended into a channel of size 60×20×30. The fibre aspect ratio, a_R, is 7.63 and the density of Newtonian fluid is set at 4.

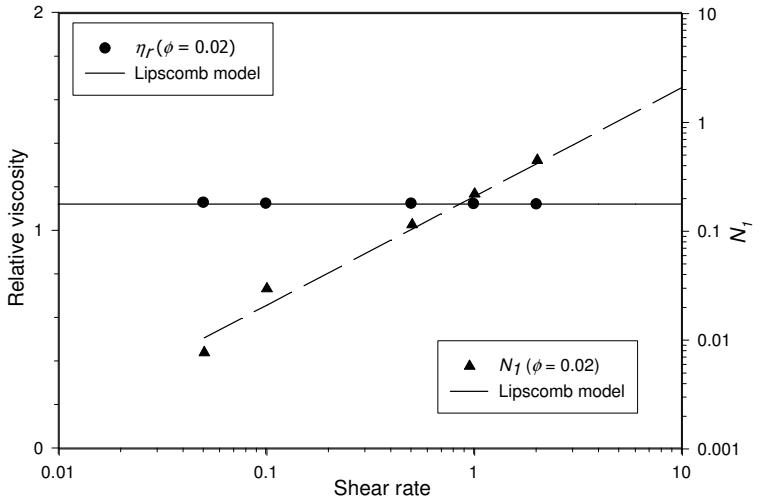

Fig. 7. Comparison of the reduced viscosity and first normal stress difference and the Lipscomb model for fibre suspension in Newtonian fluids ($\phi = 0.02$).

Several constitutive equations for suspensions have been proposed so far, a comprehensive review can be found in the work of Christopher [42] and Zirnsak et al. [43]. In 1988, Lipscomb et al. [44] have proposed a model for dilute particle suspension, which can be written for ellipsoids with high aspect ratio, as:

$$\boldsymbol{\sigma} = -P\mathbf{I} + 2\eta_0\mathbf{D} + \eta_0\phi\left(\mu_1\mathbf{D} + \mu_2\mathbf{D} : \mathbf{a}_4\right), \tag{24}$$

where μ_1 and μ_2 are rheological coefficients. Lipscomb et al. [44] suggested $\mu_1 = 2$ and $\mu_2 = \dfrac{a_R^2}{\ln(a_R)}$, and Evans [45][46] further derived from the slender-theory of Batchelor [47] to obtain $\mu_2 = \dfrac{8a_R^2}{3\ln(a_R)}$. Following Lipscomb et al. [44], we set $\mu_1 = 2$ but μ_2 is found empirically.

From those equations, the viscosity and normal stress difference can be calculated as:

$$\eta = \frac{\sigma_{21}}{\dot{\gamma}} = \eta_S\left[1 + \phi\left(2 + \mu_2 a_{1212}\right)\right], \tag{25}$$

$$N_1 - N_2 = 2\phi\eta_S\mu_2\dot{\gamma}\left(a_{1112} - 2a_{2212} + a_{3312}\right). \tag{26}$$

The non-zero normal stress differences of fibre suspensions in Newtonian solvent at steady shear flows has been reported in literature [43]. Eq. (26) shows that the normal stress in a fibre suspension is directly proportional to the shear rate, $\dot{\gamma}$,

while the first normal stress different of polymer solution is a function of $\dot{\gamma}^2$ (see Eq. (22)).

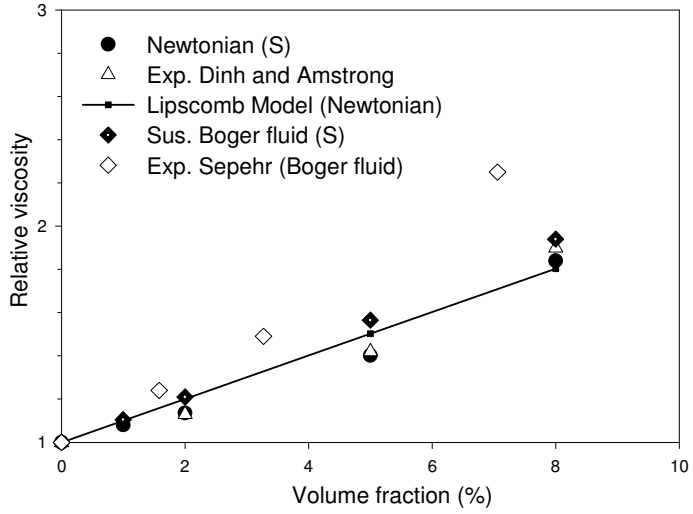

Fig. 8. Relative suspension viscosity in Newtonian (filled round) and Boger fluids (chain mass fraction of 12% at shear rate of 1.0 - filled diamond) compared with the experimental data of Dinh and Amstrong [2] (Newtonian suspending fluid) (opened triangle) as well as the experimental data of Sepehr et al. [16] (Boger suspending matrix) (opened diamond). The solid lines are the predictions of Lipscomb model for Newtonian suspending fluid.

The viscosity and first normal stress difference versus shear rate are plotted in Fig. 7. The results can be predicted well by Lipscomb model over the considered shear rates. The first normal stress difference is clearly increasing linearly with shear rate, that is in excellent agreement with Lipscomb model. The components of the orientation tensor can be calculated through our simulations and averaged over 2×10^4 time steps. The value of a_{1212} is found to be equal to 0.035 for a_R = 7.65 which reasonably agree with the value reported by Stover et al. [48] (0.012 for a_R = 32 and 0.022 for a_R = 17). This value for the orientation tensor component is independently tested by using the Folger and Tucker model [3] with the interaction coefficient C_i = 0.0028, it is found to be 0.031 (using the same programme in Ref. [16], with the ORT closure approximation defined by Wetzel and Tucker [49]). As predicted by Eq. (25), the viscosity is independent of the shear rate, the simulating results show very lightly shear thinning at highly concentrated suspensions in Fig. 7. The relative viscosity defined as $\eta_r = \eta / \eta_s$ (ratio of the suspension viscosity, η, to the solvent viscosity denoted

by η_s) is investigated for Couette flow. The results of relative viscosity are plotted in Fig. 8 and well fitted by Lipscomb model with μ_2 = 195. This value is well match with the value μ_2 = 150 found by Sepehr et al. [16] for their experiments of glass fibre suspended into PB (in their system the fibre aspect ratio is equal to 20).

3.3 *Fibre suspensions in a viscoelastic fluid*

The viscoelastic fibre suspension is simulated using the same fibres as previously discussed in section 3.1. The simulations are carried out for different volume fractions (1%, 2%, 5% and 8%) suspended into one of the above Boger fluids, namely F5-12, in a wide range of shear rates (0.05-7.5).

In Fig. 8, the viscosity of fibre suspension in Newtonian is fairly predicted by Lipscomb model which depicts the stress as a linear function of fibre volume fraction. However for Boger suspending fluid, the increase of reduced viscosity in the shear-thinning area is much larger than that in the Newtonian solvent (see Fig. 9), the same behaviour is also observed in the recent experiments of Sepehr et al. [16]. The smaller aspect ratio in our simulations (a_R = 7.63) compared to that used in the experiments (a_R = 20) may be attributed to the fact that our results are consistently smaller than experimental results.

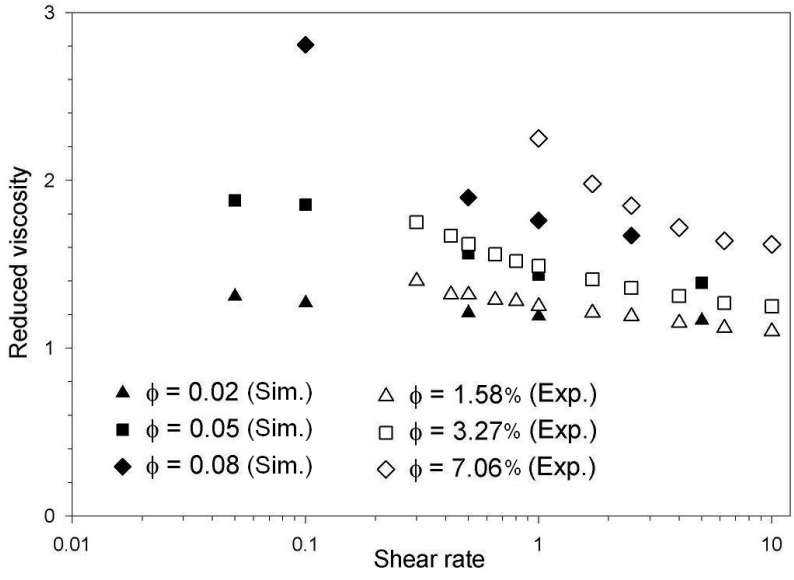

Fig. 9. Relative viscosity for a suspension in Boger fluid (chain mass fraction 12%, 5-bead chains) at different volume fractions (filled symbols), together with experimental data of Sepehr et al. [16] for fibre aspect ratio a_R = 20 in a Boger fluid which is composed of 91.0% mass of PB and 0.6% mass of polyisobutylene and 8.4% mass of kerosene (unfilled symbols).

The viscosity of a suspension in Boger fluid displays a shear thinning behaviour, which is clearly observed in some experiments [15][16], but it cannot be predicted by Lipscomb model. Fig. 9 shows that the shear thinning is stronger at higher volume fractions. It is well supported by the recent experiments of Sepehr et al. [16].

The reason for this may be due the degree orientations of fibres. Firstly, the present of polymer chains, particularly long polymer chains may augment entanglements in the suspending fluids, prevents fibre from being aligned and hence increases fibre-fibre interactions [16] at low shear rates. Secondly, the other reason may be the fibre contact behaviour that may significantly contribute to the total suspension stress and even dominating over the viscoelastic stresses [8][9]. Recently, Ausias et al. [40] proposed a direct simulation for concentrated fibre suspensions with both contact force and lubrication force. In their simulations, the fibres are allowed to touch one to another if the lubricant force is decreasingly weak, then the contact force will be replaced the lubrication force at that moment. However, fibres coming to contact are rarely observed in our simulations, hence the contact force is not considered in our simulations and it is beyond the scope of this work. Above all, Fig. 9 clearly shows that the relative viscosity of the viscoelastic fibre suspensions depends not only on the volume faction but shear rate as well. It also shows that at a critically high shear rate, the viscosity of fibre suspension in the Boger fluid approaches a plateau, where the behaviour is similar to the fibre suspension in a Newtonian fluid. It seems that there are two regions of shear rate where the behaviours of viscoelastic fibre suspensions are different. For clearer illustration, the relative viscosities of the viscoelastic fibre suspensions at two distinct shear rates are plotted in Fig. 10. One value of shear rate is chosen, e.g. 0.5, where the shear thinning of fibre suspension is observed and the other is chosen, e.g. 2.5, where relative viscosity is almost constant which is reasonably considered as a Newtonian suspension.

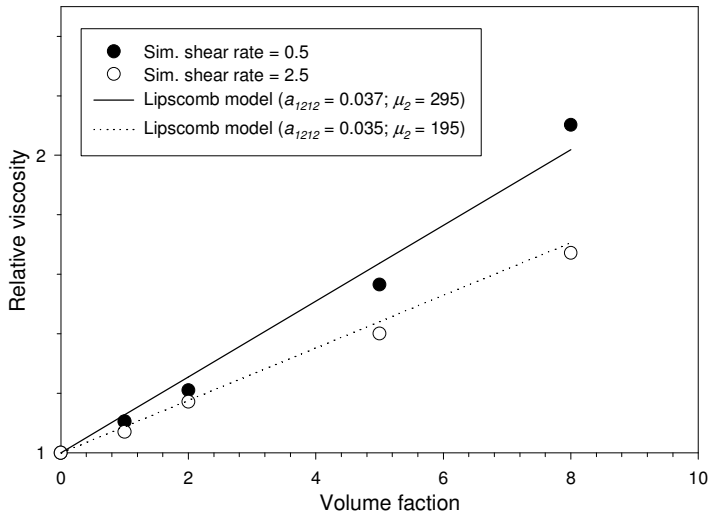

Fig. 10. The relative viscosity of fibre suspensions in a Boger fluid at different shear rates, 0.5 and 2.5. Lipscomb models are used to fit the data for both cases.

Figure 10 shows that the relative viscosity of fibre suspension in a Boger fluid at relatively high shear rate can be very well predicted by the Lipscomb model using the same parameters for fibre suspension in a Newtonian fluid. It is apparently expected since at high shear rates, polymer chains may be strongly stressed along the shear flow. Then the interaction between polymer chains and fibres is strongly reduced since most fibres are also aligned with the flow which is also observed in the fibre suspension in Newtonian fluids at high shear rates. However, at low shear rates polymer chains may prevent fibre fully aligned along the flow, particularly at high concentration of polymer where entanglement may significantly be formed among long polymer chains as discussed above. As a result, the interaction between polymer chains and fibres at low shear rates are much stronger than that at high shear rates at steady state. In Fig. 10, the data of relative viscosity at shear rate of 2.5 can be well fitted by Lipscomb model with the parameters, a_{1212} = 0.035, and μ_2 = 195 obtained from section 3.2 for the Newtonian fibre suspension. However, at the shear rate of 0.5 the Lipscomb model fairly well fits the data using the parameters a_{1212} = 0.037, and μ_2 = 295 and the error is measured about 5%. The parameter a_{1212} is calculated by averaging from our numerical results over different volume factions, i.e. 1%-8%, at the shear rate of 0.5, which is found in the range of 0.033~0.042. The value is lightly larger than the value of 0.035 found for fibre suspension in Newtonian fluid, see section 3.2. In brief, Lipscomb model can predict very well for Newtonian fibre

suspensions and the viscoelastic fibre suspension at high shear rates, but not for low shear rates. It seems that for highly accurate results for fibre suspension in viscoelastic fluid at low shear rates, the value of a_{1212} should be taken the interaction between fibres and polymer chains into account rather than just a constant as Newtonian fibre suspensions.

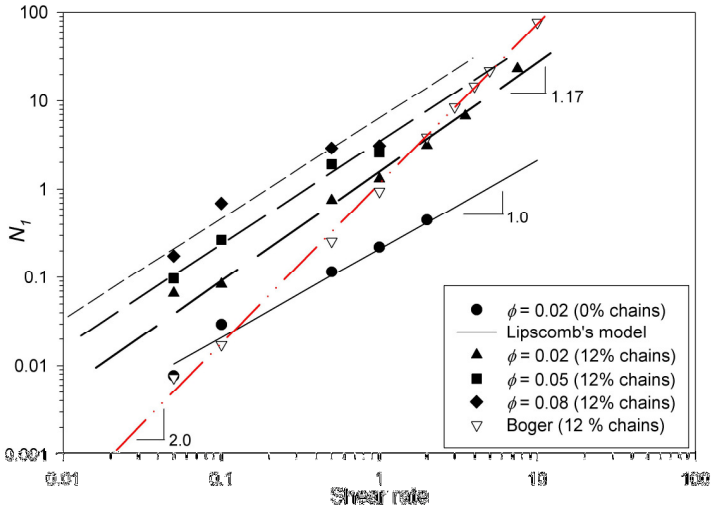

Fig. 11. Comparison of the first normal stress difference of suspensions in Newtonian and Boger fluids together with Lipscomb model. The slope of N_1 of suspensions in a Newtonian is 1.0 as good as predicted by Lipscomb model (solid line), but the slope of N_1 of suspensions in Boger fluid is about 1.17 (dash line) and the slope of N_1 of unfilled Boger fluid is 2.0 as predicted by Oldroyd-B model (dotted-dash line).

The first normal stress difference of suspensions in Newtonian and Boger fluids is plotted in Fig. 11. The first normal stress difference of suspension in Newtonian is in good agreement with Lipscomb model which is predicted N_1 is a linear function of shear rate. This is well supported by the literature data [43] [50][51]. The value of first normal stress difference in Boger fluids is found more pronounced than that in Newtonian fluid. Goto et al. [51] reported that the slopes of N_1 in log-log scale versus shear rate vary in the range of 0.5 and 1.2 using different sorts of fibres, fibre concentrations and fibre aspect ratios. They also observed that increasing the aspect ratio of fibre will increase the absolute value of N_1 but decrease the slope of N_1 in log-log plot. Furthermore, increasing the volume fraction at a given aspect fibre ratio, the same affect is seen. This trend is again confirmed in our simulations, Fig. 11. However, at high shear rates and for concentrated suspensions, DPD results may not be accurate since the DPD thermostat may not work well at strong flows. Interestingly we found that the slope of 1.17 fits well the data of the suspension in Boger fluid (ϕ = 0.02), that

value is in the upper range found by Goto et al. [51]. In recent work of Sepehr et al. [16], N_1 is detected to be a quadratic function of shear rate as the same as for the unfilled Boger fluid.

4. Conclusions

A DPD model of fibre suspensions in Newtonian and viscoelastic fluids is presented. Linear chains are used to model viscoelastic fluid, which is a good model for Boger fluid. Simulating results for the viscoelastic fluid are in excellent agreement with the Oldroyd-B model in shear flows. Simulations of fibre suspensions are carried out in Couette flow. The viscosity of fibre suspensions in Newtonian fluids is obsvered almost constant over the shear rate range considered, while the normal stress difference is a linear function of shear rate. However in Boger suspending fluids, the increase of viscosity and first normal stress difference is more pronounced than that in Newtonian fluids.

In general, Lipscomb model is very good in predicting the viscosity of Newtonian suspension for a wide range of shear rates and fibre volume fractions. However, it is incapable to capture the shear thinning behaviour of fibre suspension in Boger fluids. Lipscomb model may be used to predict such suspensions at low concentration and high shear rate. The slope of first normal stress difference for suspensions in Boger fluids is found about 1.17 (for $\phi = 0.02$) which is consistent with Goto et al.'s [51] results, but less than the quadratic value reported in Sepehr et al.'s experiments [16]. The first normal stress different of suspensions in Newtonian fluid is well fitted by a linear function of shear rate as predicted by Lipscomb model.

A simple parallel algorithm is proposed to enhance the computational capacity; however more effort in future is needed to increase the efficiency of the parallel algorithm.

Acknowledgments

We would thank Professor Charles Tucker for permission to use the program in calculating the closure approximations.

References:

[1] W.J. Milliken, R.L. Powell, Short-fiber suspensions; C.L. Tucker III, S.G. Advani, Processing of Short-Fiber Systems, Flow and Rheology in Polymer Composites Manufacturing, edited by S.G. Advani, V. 10 Composite Material Series, Elsevier, 1994

[2] S.H. Dinh, R.C. Armstrong, A rheological equation of state for semi-concentrated fiber suspensions, J. Rheol. 28 (1984) 207.

[3] F.P. Folgar, C.L. Tucker, Orientation behavior of fibers in concentrated suspensions, J. Reinforced Plast. Composites 3 (1984) 98.

[4] Y. Yamane, Y. Kaneda, M. Doi, Numerical simulation of semi-dilute suspensions of rodlike particles in shear flow, J. Non-Newtonian Fluid Mech. 54 (1994) 405.

[5] Y. Yamane, Y. Kaneda, M. Doi, The effect of interaction of rodlike particles in semi-dilute suspensions under shear flow, J. Phys. Soc. Jpn. 64 (1995) 3265.

[6] N. Phan-Thien, X.-J. Fan, R.I. Tanner, R. Zheng, Folgar-Tucker constant for a fibre suspension in a Newtonian fluid, J. Non-Newtonian Fluid Mech. 103 (2002) 251.

[7] D.D. Josehp, Y.J. Liu, Orientation of long bodies falling in a viscoelastic liquid, J. Rheol. 37 (1993) 961.

[8] Y. Iso, D.L. Koch, C. Cohen, Orientation in simple shear flow of semi-dilute fiber suspensions, 1. Weakly Elastic Fluids, J. Non-Newtonian Fluid Mech. 62 (1996) 115.

[9] Y. Iso, D.L. Koch, C. Cohen, Orientation in simple shear flow of semi-dilute fiber suspensions: II. Highly elastic fluids, J. Non-Newtonian Fluid Mech. 62 (1996) 135.

[10] N. Phan-Thien, X.J. Fan, Viscoelastic mobility problem using a boundary element method, J. Non-Newtonian Fluid Mech. 105 (2002) 131.

[11] Y.Chan, J.L. White, Y. Oyanagi, A fundamental study of the rheological properties of glass-fibre-reinforced polyethylene and polystyrene melts, J. Rheol. 33 (1978) 507.

[12] E. Ganani, R.L. Powell, Rheolocigal properties of Rodlike Particles in a Newtonian and a Non-Newtonian Fluid, J. Rheol. 30 (1986) 995.

[13] J. Azaiez, Constitutive equations for fiber suspensions in viscoelastic media, J. Non-Newtonian Fluid Mech. 66 (1996) 35.

[14] A. Ramazani, A. AitKadi, M. Grmela, Rheological modelling of short fiber thermoplastic composites, J. Non-Newtonian Fluid Mech. 73 (1997) 241.

[15] A. Ramazani, A. Ait-Kadi, M. Grmela, Rheology of fibre suspensions in viscoelastic media: Experiments and model predictions, J. Rheol. 45 (2001) 945.

[16] M. Sepehr, P.J. Carreau, M. Moan, G. Ausias, Rheological properties of short fiber model suspensions, J. Rheol. 48 (2004) 1023.

[17] P.J. Hoogerbrugge, J.M.V.A. Koelman, Simulating microscopic hydrodynamic phenomena with dissipative particle dynamics, Europhys. Lett. 19 (1992) 155.

[18] J.M.V.A. Koelman, P.J. Hoogerbrugge, Dynamic simulations of hard-sphere suspensions under steady shear, Europhys. Lett. 21 (1993) 363.

[19] D. Duong-Hong, G. Chaidron, S. Nigen, S.H.S. Dave, N. Phan-Thien, C.L Teo, E. Burdet and S.P. Joseph, Numerical Simulation of Soft Solids by the

Versatile Network Approach:Application to a Neuroprobe entering a brain tissue, Proc. 14th International Congress Rheology, Korea 2004, CR22.
[20] A. Chatterjee, L.-M. Wu, Predicting rheology of suspensions of spherical and non-spherical particles using dissipative particle dynamics (DPD): methodology and experimental validation, Molecular Simulation 34 (3) (2008) 243.
[21] D. Duong-Hong, J-S. Wang, G-R. Liu, Y. Z. Chen, J. Han, N.G. Hadjiconstantinou, Dissipative particle dynamics simulations of electroosmotic flow in nano-fluidic devices, Microfluidics and Nanofluidics 4 (2008) 219.
[22] D. Duong-Hong, J-S. Wang, G-R. Liu, Y. Z. Chen, J. Han, N.G. Hadjiconstantinou, Realistic Simulations of Combined DNA Electrophoretic and Electroosmotic Flows in Nano-Fluidic Devices, Electophoresis 29 (2008) 4880.
[23] A.G. Schlijper, P.J. Hoogerbrugge, C. W. Manke, Computer Simulation of dilute polymer solution with the dissipative particle dynamics method, J. Rheol. 39 (1995) 567.
[24] S. Chen, N. Phan-Thien, X.J. Fan, B.C. Khoo, Dissipative particle dynamics simulation of polymer drops in a periodic shear flow, J. Non-Newtonian Fluid Mech. 118 (2004) 65.
[25] X.J. Fan, N. Phan-Thien, S. Chen, X.H. Wu, T.Y. Ng, Simulating flow of DNA suspension using dissipative particle dynamics, Phys. Fluids 18 (2006) 063102.
[26] N.S. Martys, R.D. Mountain, Velocity Verlet algorithm for dissipative-particle-dynamics-based models of suspensions, Phys. Rev. E 59 (1999) 3733.
[27] S. Yamamoto, T. Matsuoka, A method for dynamic simulation of rigid and flexible fibers in a flow field, J. Chem. Phys. 98 (1993) 644.
[28] S. Yamamoto, T. Matsuoka, Dynamic simulation of fibers suspension in shear flow, J. Chem. Phys. 102 (1994) 2254.
[29] P. Español and P. Warren, Statistical Mechanics of Dissipative Particle Dynamics, Europhys. Lett. 30 (1995) 191.
[30] R. D. Groot, P. B. Warren, Dissipative particle dynamics: bridging the gap between atomic and mesoscopic simulation, J. Chem. Phys. 107 (1997) 4423.
[31] C. Marsh, Theoretical Aspect of Dissipative Particle Dynamics, PhD thesis, University of Oxford, 1998.
[32] X.J. Fan, N. Phan-Thien, S. Chen, X.H. Wu, T.Y. Ng, Simulation flow of DNA suspension using dissipative particle dynamics, Phys. Fluid 18 (2006) 063102.
[33] J.H. Irving, J.G. Kirkwood, The statistical mechanics of transport processes IV. The equation of hydrodynamics, J. Chem. Phys. 18 (1950) 817.
[34] M. Revenga, I. Zúñiga, P. Español, Boundary condition in dissipative particle dynamics, Computer Phys. Commun. 121 (1999) 309.
[35] D. Duong-Hong, N. Phan-Thien, X.J. Fan, An implementation of no-slip boundary conditions in DPD, Comput. Mech. 35 (2004) 24.
[36] I.P. Omelyan, On the numerical integration of motion for rigid polyatomics: The modified quaternion approach, Computers in Physics 12 (1998) 97.
[37] D.C. Rapaport, The Art of Molecular Dynamics Simulation, Cambridge University Press, Cambridge, 1995.

[38] G. Strang, Introduction to linear algebra**,** Wellesly, MA: Wellesley-Cambridge, 2003.
[39] N. Phan-Thien, S. Kim, Micro Structures in Elastic Media: principles and computational methods, New York: Oxford University Press, 1994.
[40] G. Ausias, X.J. Fan, R.I. Tanner, Direct simulation for concentrated fibre suspensions in transient and steady state shear flows, J. Non-Newtonian Fluid Mech. 135 (2006) 46.
[41] R.B. Bird, R.C. Armstrong, O. Hassager, Dynamics of Polymeric liquids: Vol 1: Fluid Mechanics, 2nd edition, New York, John Wiley & Sons, 1987.
[42] J.S.P. Christopher, The rheology of fibre suspensions, J. Non-Newtonian Fluid Mech. 87 (1999) 369.
[43] M.A. Zirnsak, D.U. Hur, D.V. Boger, Normal stresses in fiber suspensions, J. Non-Newtonian Fluid Mech. 54 (1994) 153.
[44] G.G. Lipscomb II, M.M. Denn, D.U. Hur, D.V. Boger, The flow of fibre suspensions in complex geometry, J. Non-Newtonian Fluid Mech. 26 (1988) 297.
[45] J.G. Evans, The flow of a suspension of force-free rigid rods in a Newtonian fluid, Ph.D. Thesis, Cambridge University, Cambridge, 1975.
[46] J.G. Evans, The effect of non-Newtonian properties of a suspension of rod-like particles on flow fields, in: J.R.A. Pearson, K. Walters, J.F. Hutton (Eds.), Theoretical Rheology, Halstead Press, New York, 1975.
[47] G.K. Batchelor, The stress system in a suspension of force-free particles, J. Fluid Mech. 41 (3) (1970) 545.
[48] C.A. Stover, D.L. Koch, C. Cohen, Observation of fiber orientation in simple shear flow of semi-dilute suspensions, J. Fluid Mech. 238 (1992) 277.
[49] E.D. Wetzel, C.L. Tucker III, Area tensors for modeling microstructure during laminar liquid-liquid mixing, Int. J. Multiphase Flow 25 (1999) 35.
[50] L. F. Carter, ‘‘A study of the rheology of suspensions of rod-shaped particles in a Navier–Stokes liquid,’’ Ph.D. Dissertation, University of Michigan, Ann Arbor, MI, 1967. L. F. Carter, and J. D. Goddard, ‘‘A rheological study of glass fibers in a Newtonian fluid,’’ NASA Report No. N67-30073, 1967.
[51] S. Goto, H. Nagazono, H. Kato, The flow behavior of fiber suspensions in Newtonian fluids and polymers solutions. II. Capillary flow, Rheol. Acta. 25 (1986) 246.